Human Molecular Genetics, 2021, Vol. 30, No. 22 2149–2160

https://doi.org/10.1093/hmg/ddab179
Advance Access Publication Date: 3 July 2021
General Article

GENERAL ARTICLE

Stress modulates Ahi1-dependent nuclear localization of ten-eleven translocation protein 2

Qian Zhang[1,2], Qicheng Hu[2], Junjie Wang[2], Zhigang Miao[2,†], Ziyi Li[3], Yuwen Zhao[4], Bo Wan[2], Emily G. Allen[4], Miao Sun[5], Peng Jin[4,*,‡] and Xingshun Xu[1,2,6,*]

[1]Department of Neurology, The First Affiliated Hospital of Soochow University, Suzhou City 215006, China, [2]Institute of Neuroscience, Soochow University, Suzhou City 215123, China, [3]Department of Biostatistics, The University of Texas MD Anderson Cancer Center, Houston, TX 77030, USA, [4]Department of Human Genetics, Emory University School of Medicine, Atlanta, GA 30315, USA, [5]The Institute of Fetology, The First Affiliated Hospital of Soochow University, Suzhou City 215006, China and [6]Jiangsu Key Laboratory of Neuropsychiatric Diseases, Soochow University, Suzhou, Jiangsu 215123, China

*To whom correspondence should be addressed. Tel: 404-727-3729 (Office); 404-727-7564 (Lab); Fax: 404-727-5408; Email: peng.jin@emory.edu and xingshunxu@suda.edu.cn

Abstract

Major depression disorder is one of the most common psychiatric diseases. Recent evidence supports that environmental stress affects gene expression and promotes the pathological process of depression through epigenetic mechanisms. Three ten-eleven translocation (Tet) enzymes are epigenetic regulators of gene expression that promote 5-hydroxymethylcytosine (5hmC) modification of genes. Here, we show that the loss of Tet2 can induce depression-like phenotypes in mice. Paradoxically, using the paradigms of chronic stress, such as chronic mild stress and chronic social defeat stress, we found that depressive behaviors were associated with increased Tet2 expression but decreased global 5hmC level in hippocampus. We examined the genome-wide 5hmC profile in the hippocampus of Tet2 knockout mice and identified 651 dynamically hydroxymethylated regions, some of which overlapped with known depression-associated loci. We further showed that chronic stress could induce the abnormal nuclear translocation of Tet2 protein from cytosol. Through Tet2 immunoprecipitation and mass spectrum analyses, we identified a cellular trafficking protein, Abelson helper integration site-1 (Ahi1), which could interact with Tet2 protein. Ahi1 knockout or knockdown caused the accumulation of Tet2 in cytosol. The reduction of Ahi1 protein under chronic stress explained the abnormal Ahi1-dependent nuclear translocation of Tet2. These findings together provide the evidence for a critical role of modulating Tet2 nuclear translocation in regulating stress response.

Introduction

Major depression disorder (MDD) is one of the most common psychiatric diseases. Depressive symptoms can persist for weeks or a lifetime, and even if cured, there is a risk of recurrence throughout the lifespan (1). The pathogenesis of MDD remains unclear and is considered to be related to biological, psychological and social environment factors (2,3). Although many studies have shown that genetic mutations in stress-related genes such

†Zhigang Miao, http://orcid.org/0000-0002-9258-671X
‡Peng Jin, http://orcid.org/0000-0001-6137-6659
Received: April 7, 2021. **Revised:** June 8, 2021. **Accepted:** June 24, 2021

as CRHR1, BDNF, NMDA and SNAP25 are associated with MDD (4–7), genetic factors do not fully explain the mechanism of depression (8). Recent evidence supports that environmental stress affects gene expression and promotes the pathological process of depression through epigenetic mechanisms (9–11). Among epigenetic mechanisms, DNA methylation is the most widely studied and is considered to be highly involved with the mechanism of MDD (12,13). Alternatively, DNA demethylation may also be associated with MDD, and several recent studies support this notion (14–16). As a mechanism of demethylation, 5-hydroxymethylcytosine (5hmC) is found to be oxidized from 5-methylcytosine (5mC) by ten-eleven translocation (Tet) enzymes Tet1/2/3 (17,18). A decrease in global 5hmC has been found in peripheral leukocytes of patients with MDD compared with healthy controls (16). Recent evidence also suggests that 5hmC is implicated in the molecular mechanisms of drugs with antidepressant-like effects (19,20). Therefore, Tet enzymes could be genetic modifiers responsible for the different phenotypes of MDD.

Adult mice with loss of Tet1 in nucleus accumbens (NAc) neurons exhibit resistance to chronic social defeat stress (CSDS), and a selective reduction of Tet1 expression in the NAc was observed in CSDS-susceptible mice, but not in CSDS-resistant mice (21). Neuronal regulatory genes such as Npas4, c-Fos, Arc, Egr2 and Egr4, which play important roles in mediating synaptic plasticity and cognition, were significantly downregulated in the hippocampus of Tet1 KO mice (22). It has been shown that Tet3 homozygous deletion leads to abnormal demethylation of the paternal Oct4 and Nanog genes, which ultimately reduces fetal survival (23). Increased anxiety-like behavior and impaired hippocampal spatial orientation were observed in neuronal Tet3-deficient mice (24). Our previous study showed that Tet1/HIF1a-mediated gene 5hmC modification was involved in the response to environmental stress (25). These studies suggest that Tet1 and Tet3 play different roles in various psychiatric disorders, despite their similar enzymatic actions.

Here we show that the loss of Tet2 can induce depression-like phenotypes in mice. Using the paradigm of chronic stress, we found that depressive behaviors were associated with increased Tet2 expression but decreased global 5hmC levels in hippocampus. We further found that chronic stress could induce the abnormal nuclear translocation of Tet2 protein from the cytosol. We identified a cellular trafficking protein, Abelson helper integration site-1 (Ahi1), which could interact with Tet2 protein and modulate the nuclear translocation of Tet2. Our analyses demonstrate that Ahi1-mediated nuclear translocation of Tet2 plays a critical role in regulating stress response.

Results

Tet2 deficiency in mice causes depression-like phenotypes

To investigate the important role of Tet2 in the central nervous system, we generated Tet2 conditional knockout (CKO) mice by crossing loxP-flanked Tet2 mice with Nestin-Cre mice (Fig. 1A). Tet2 protein levels were significantly decreased in the brain as shown in Figure 1B ($P < 0.05$), but normal distribution of Tet2 was seen in the heart, liver, spleen, lung, kidney and muscle (Supplementary Material, Fig. S1A). The forced swim test (FST), tail suspension test (TST) and novelty-suppressed feeding test (NSFT) are classical methods to evaluate depressive-like behaviors (26). Tet2 CKO mice displayed depression-like behaviors including increased immobility time in the FST ($P < 0.05$, Fig. 1C) and TST ($P < 0.05$, Fig. 1D), and increased latency to feed in the NSFT ($P < 0.05$, Fig. 1E).

To further confirm the role of Tet2 in the depression-like behaviors that we observed, we stereotactically injected adeno-associated virus (AAV) carrying Cre to specifically knockdown Tet2 in the hippocampus of homozygous loxP-flanked Tet2 mice (Fig. 1F). At 21 days after injection, immobility time in FST (Fig. 1G) and TST (Fig. 1H) markedly increased in AAV-Cre–treated mice compared with control virus-treated mice. EGFP signal was observed in the hippocampus of both virus-treated mice (Supplementary Material, Fig. S1B). In addition, we treated Cre^{ERT2} $Tet2^{fl/fl}$ mice for 5 days with tamoxifen to delete Tet2 (Fig. 1I). At seven days after the last injection, tamoxifen-treated mice had an increased immobility time in FST and TST compared with the sham group (Fig. 1J and K). Therefore, the loss of Tet2 could lead to depression-like behaviors.

Tet2 protein increases in hippocampus upon stress exposure

Because Tet2 deficiency caused depression-like behaviors, we investigated whether Tet2 protein levels were altered in stress-induced depressive mice. After chronic mild stress (CMS), immobility time in FST ($P < 0.01$, Fig. 2A) and TST ($P < 0.01$, Fig. 2B) was significantly increased in stressed mice; consumed sucrose water was also reduced in stressed mice ($P < 0.01$, Fig. 2C). At the same time, Tet2 mRNA levels were markedly increased in the hippocampus of stressed mice ($P < 0.01$, Fig. 2D). Tet2 protein levels were also significantly elevated in the hippocampus of stressed mice compared with control mice ($P < 0.05$, Fig. 2E). Surprisingly, in contrast to the increase in Tet2 levels, global 5hmC levels in the hippocampus of stressed mice were significantly decreased ($P < 0.05$, Fig. 2F and G). Further, we examined Tet2 and 5hmC levels in CSDS-treated mice and obtained similar results (Supplementary Material, Fig. S2). These findings together demonstrate that environmental stress can increase the expression of Tet2 but decrease the overall abundance of 5hmC.

The loss of Tet2 alters the 5hmC landscape

Since the loss of Tet2 can cause a global decrease of 5hmC, we further examined genome-wide 5hmC profiles in the hippocampus of Tet2 CKO mice by using a previously established 5hmC capture method, combined with high-throughput sequencing (25). Genomic annotation of DhMRs revealed that Tet2 CKO-induced DhMRs had about 62% (Fig. 3A and Supplementary Material, Table S1) of the regions associated with intragenic regions. Furthermore, Tet2 CKO-induced DhMRs showed the highest enrichment at exons compared with expected values (Fig. 3A). More bins had low 5hmC reads in Tet2 CKO mice compared with those from WT mice (Fig. 3B). The Tet2 CKO versus WT group had a total of 651 DhMRs and mapped to 461 unique human genes. We obtained the genes associated with depression (27), and overlapped the disease-related genes with our identified genes. There were 31 overlapping regions between Tet2 CKO-induced DhMR-associated genes and depression-associated genes (Fig. 3C). The KEGG pathway analysis showed that the Tet2 CKO-induced DhMRs were significantly enriched in pathways in glutamatergic synapse (28), oxytocin signaling pathway (29) and circadian entrainment (30) (Fig. 3D), which have been reported to be associated with depression. Meanwhile, Gene Ontology (GO) analysis showed that the Tet2

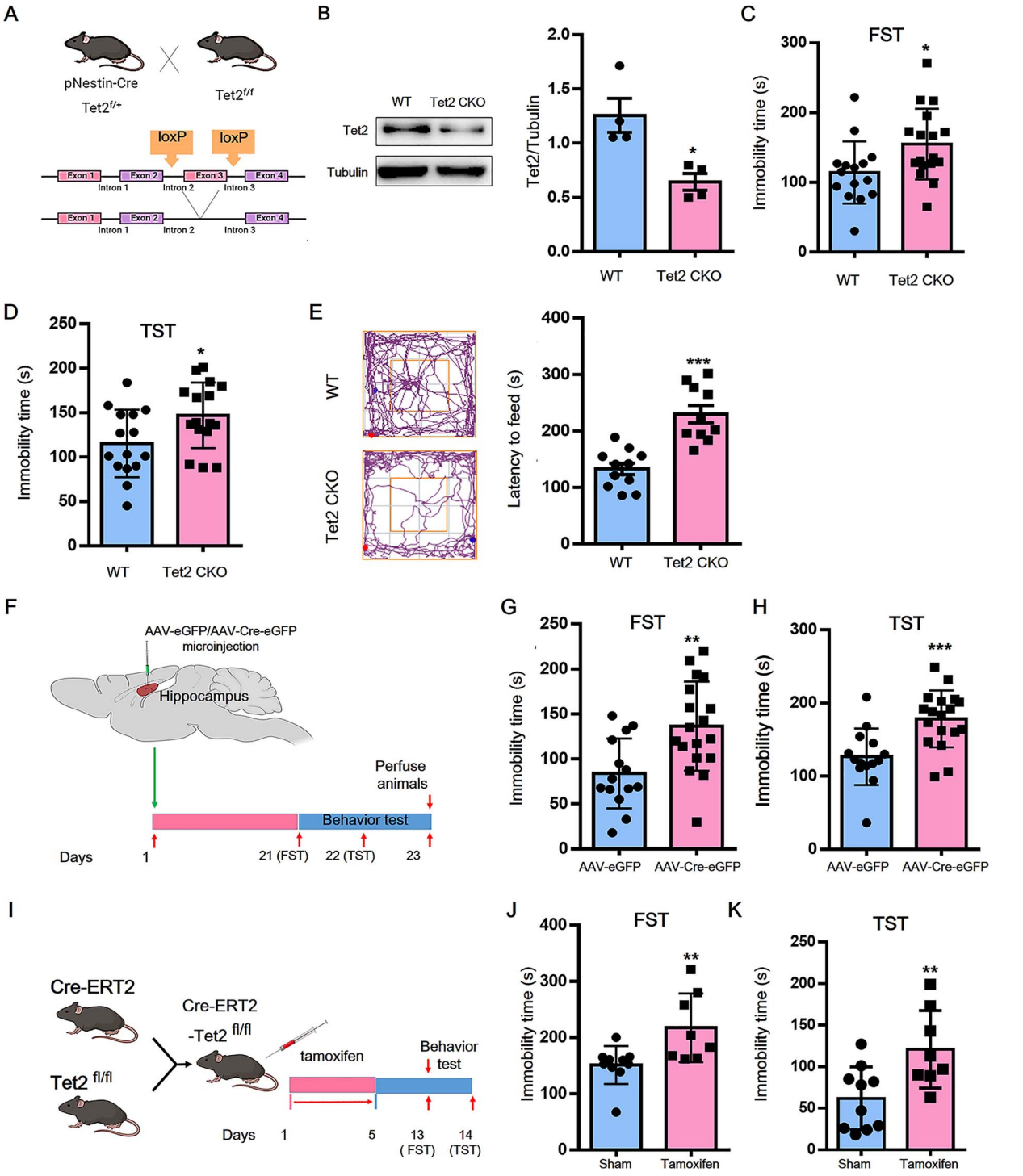

Figure 1. The loss of Tet2 in mice results in severe depression-like behavior. (**A**) pNestin-Cre-Tet2 $^{f/+}$ mice were crossed with Tet2 $^{f/f}$ mice to obtain Tet2 CKO mice. (**B**) Representative western blots of Tet2 in hippocampus of WT and Tet2 CKO mice, $N = 4$, two-tailed Student's t test, $^{*}P < 0.05$, $t = 3.515$, $df = 6$, vs WT group. The data of WT group is represented by dots and Tet2 CKO group is represented by squares. (**C**) Forced swimming test (FST) occurred with Tet2 CKO and their littermate control mice, $N = 15, 17$, two-tailed Student's t test, $^{*}P < 0.05$, $t = 2.4$, $df = 30$, vs WT group. The data of WT group is represented by dots and Tet2 CKO group is represented by squares. (**D**) Tail-suspension test (TST) occurred with Tet2 CKO and their littermate control mice, $N = 15, 16$, two-tailed Student's t test, $^{*}P < 0.05$, $t = 2.341$, $df = 29$, vs WT group. The data of WT group is represented by dots and Tet2 CKO group is represented by squares. (**E**) Novelty-suppressed feeding test (NSFT) occurred with Tet2 CKO and their littermate control mice, $N = 11, 10$, two-tailed Student's t test, $^{***}P < 0.001$, $t = 5.296$, $df = 19$, vs WT group. The data of WT group is represented by dots and Tet2 CKO group is represented by squares. (**F**) Timeline of experimental procedure in the AAV-Cre-induced hippocampal Tet2 KO mouse. (**G**) FST and (**H**) TST occurred with Tet2 $^{floxp/floxp}$ –AAV-eGFP and Tet2 $^{floxp/floxp}$ –AAV-Cre-eGFP mice. AAV-eGFP, adenovirus serotype 5 expressing enhanced green fluorescent protein; AAV-Cre-eGFP, adenovirus serotype 5 Cre. $N = 14, 18$, two-tailed Student's t test, $^{**}P < 0.01$, $t = 3.216$, $df = 30$, $^{***}P < 0.001$, $t = 3.738$, $df = 30$, vs AAV-eGFP group. The data of AAV-eGFP group is represented by dots and AAV-Cre-eGFP group is represented by squares. (**I**) Timeline of experimental procedure in the tamoxifen-induced Tet2 KO mouse. (**J**) FST and (**K**) TST occurred with Tet2 $^{floxp/floxp}$ –sham and Tet2 $^{floxp/floxp}$ –tamoxifen mice. $N = 10, 8$, two-tailed Student's t test, $^{**}P < 0.01$, $t = 2.931$, $df = 16$, $^{**}P < 0.01$, $t = 2.973$, $df = 16$, vs Tet2 $^{floxp/floxp}$ –sham group. The data of Sham group is represented by dots and Tamoxifen group is represented by squares. Data are expressed as mean ± S.E.M.

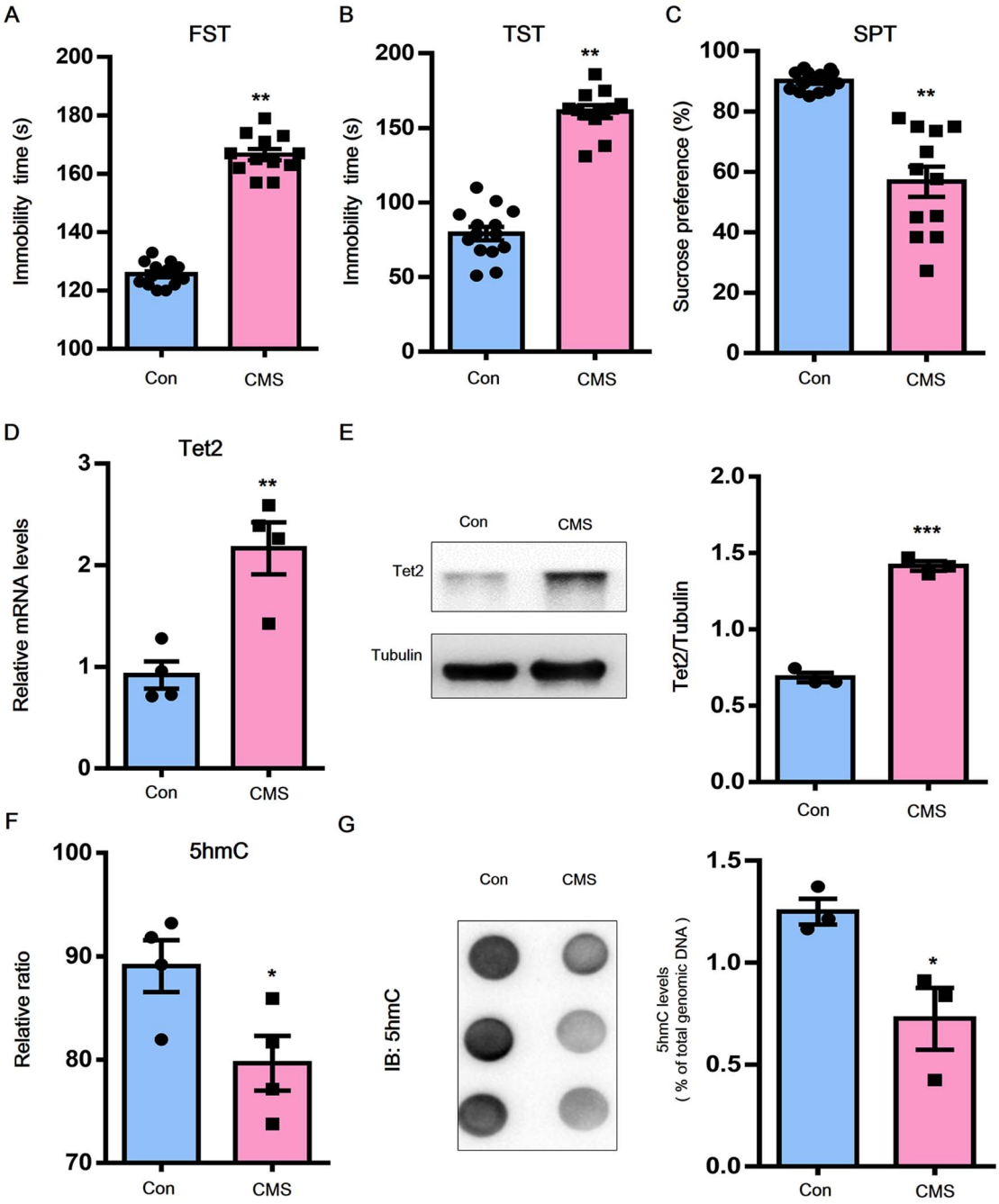

Figure 2. Tet2 expression changes inversely to 5hmC abundance in hippocampus of chronic mild stress (CMS) models. (**A–C**) Behavioral tests were performed after experimental procedure. (A) FST, $N = 14, 12$, two-tailed Student's t test, $^{**}P < 0.01$, $t = 12.96$, $df = 24$; (B) TST, $N = 14, 12$, two-tailed Student's t test, $^{**}P < 0.01$, $t = 19.27$, $df = 24$; (C) 1% sucrose preference test (SPT), $N = 14, 12$, two-tailed Student's t test, $^{**}P < 0.01$, $t = 7.059$, $df = 24$. (**D**) Levels of Tet2 mRNA were increased in the hippocampus of CMS mice. $N = 4$, two-tailed Student's t test, $^{**}P < 0.01$, $t = 4.322$, $df = 6$. (**E**) Levels of Tet2 protein were increased in the hippocampus of CMS mice. $N = 3$, two-tailed Student's t test, $^{***}P < 0.001$, $t = 16.77$, $df = 4$. (**F**) Global 5hmC levels from genomic DNA extracted from hippocampus of CMS mice were quantified by 5hmC ELISA. N=4, two-tailed Student's t test, $^{*}P < 0.05$, $t = 2.581$, $df = 6$. (**G**) Global 5hmC levels from genomic DNA extracted from hippocampus of CMS mice were quantified by 5hmC dot blot. $N = 3$, two-tailed Student's t test, $^{*}P < 0.05$, $t = 3.2$, $df = 4$. Data are expressed as mean ± S.E.M., vs control group.

CKO-induced DhMRs were mainly enriched in genes related to regeneration, synapse organization and postsynaptic density assembly (Fig. 3E). In concordance with these 5hmC-seq results, a reduction of postsynaptic density protein 95 (PSD95) was observed in the dorsal hippocampus by immunofluorescence (Supplementary Material, Fig. S1C). In addition, we detected two synapse-associated proteins, neurofilament protein 200 (NF200) and microtubule-associated protein 2 (MAP2). Immunofluorescence staining showed that both NF200 and MAP2 in the hippocampus of Tet2 CKO mice were significantly lower than that of control mice (Supplementary Material, Fig. S1D and E).

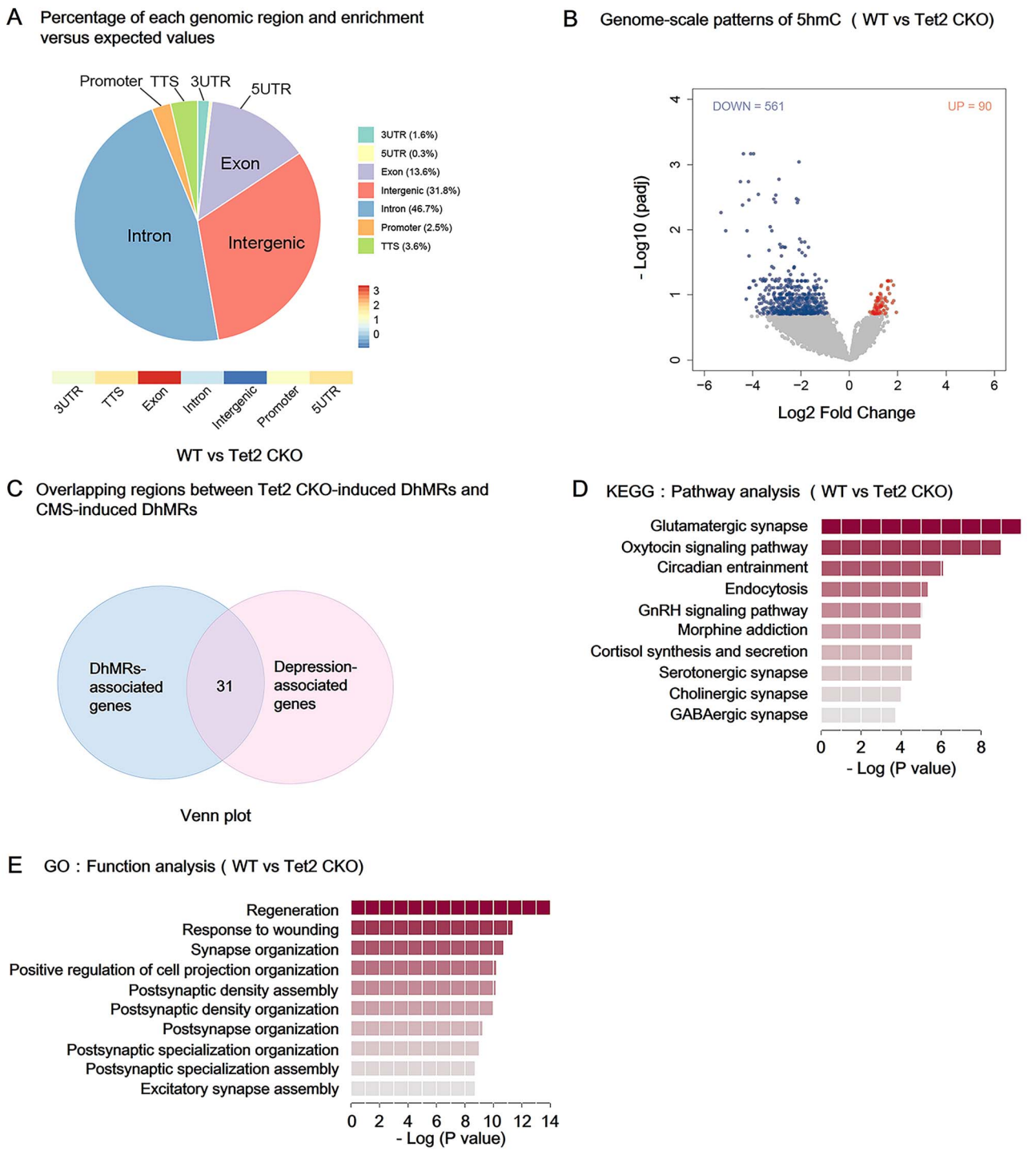

Figure 3. The loss of Tet2 leads to dynamic change of 5hmC in hippocampus. (**A**) Genomic annotation of Tet2 CKO–induced DhMRs to demonstrate their percentage of each genomic region and enrichment versus expected values. (**B**) A volcano plot of Tet2 CKO-induced DhMRs. (**C**) A Venn diagram shows 31 overlapping regions between Tet2 CKO-induced DhMRs and depression-associated genes. (**D**) KEGG analysis on pathways with Tet2 CKO-induced DhMRs. (**E**) GO analysis on biological process with Tet2 CKO-induced DhMRs.

Tet2 nuclear translocation is reduced upon stress exposure

Under physiological conditions, Tet2 is predominantly localized in the nucleus to maintain its catalytic and non-catalytic functions (31). Therefore, we examined if the cellular distribution of Tet2 under chronic stress conditions could explain the global decrease of genomic 5hmC. Immunofluorescent staining showed Tet2 mainly distributed in the nuclear area; however, under chronic stress, nuclear Tet2 was significantly reduced and diffuse Tet2 was found in the cytosol (Fig. 4A). Quantitative analysis of Tet2 immunofluorescence intensity also showed the marked decrease of nuclear Tet2 in the hippocampus of stressed

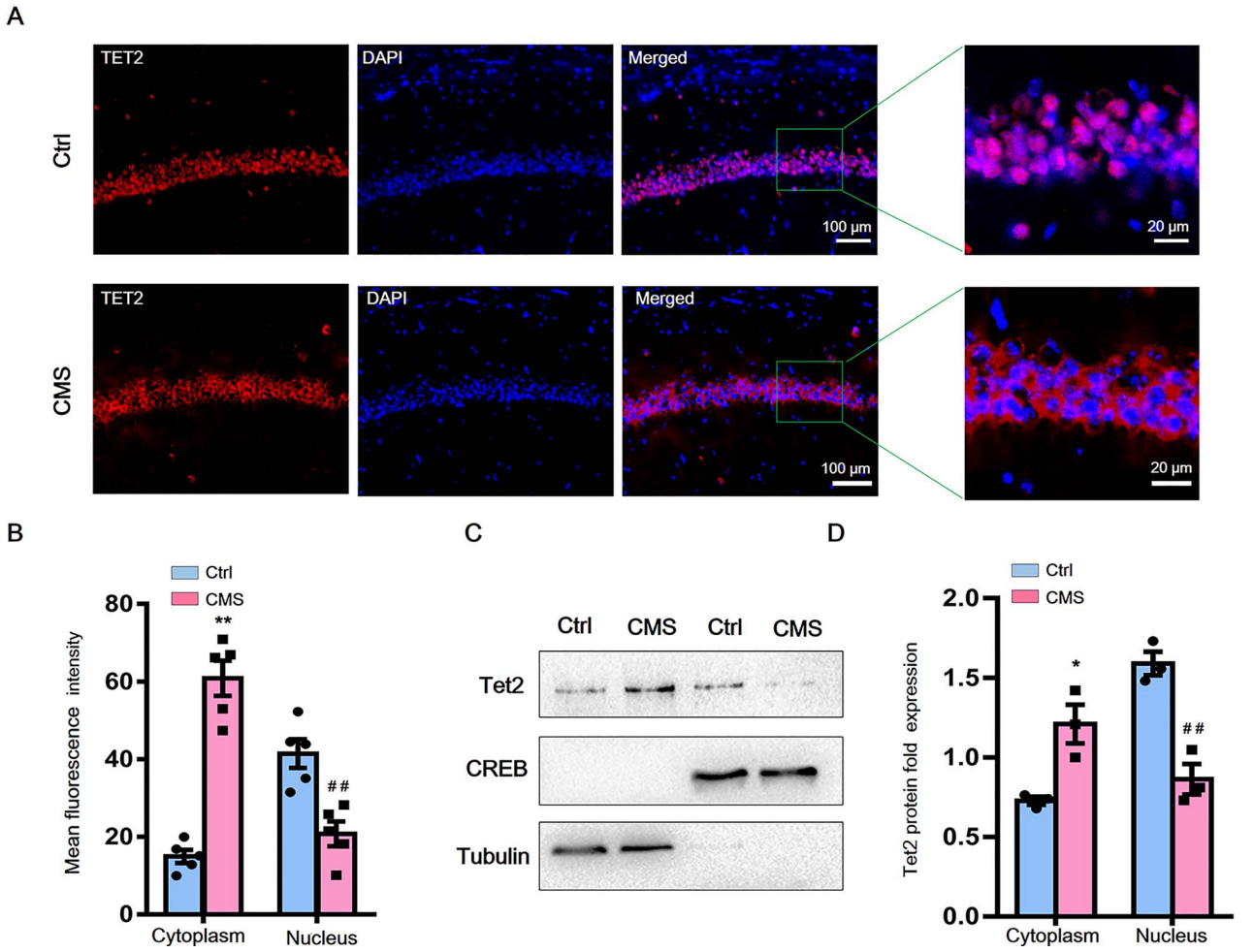

Figure 4. Increased Tet2 in the cytoplasm of the hippocampus of CMS mice. (**A**) Control and CMS brains stained for Tet2 (red) and DAPI (blue) reveal Tet2 mislocalization into the cytoplasm in CA1, Scale bar, 100 μm (left), 20 μm (right). (**B**) Quantification of nuclear and cytoplasmic Tet2 protein intensity in CA1. The data of Con group is represented by dots and CMS group is represented by squares. $N = 5$, two-tailed Student's t test, $^{**}P < 0.01$, $t = 9.514$, $df = 8$, vs control-Cytoplasm group, $^{\#\#}P < 0.01$, $t = 4.239$, $df = 8$, vs control-Nucleus group. (**C, D**) Separation of the nuclear and cytoplasmic fractions confirms Tet2 accumulation in the cytoplasm of hippocampus of CMS mice. Tubulin and CREB served as cytoplasmic and nuclear markers, respectively. The data of Con group is represented by dots and CMS group is represented by squares. $N = 3$, two-tailed Student's t test, $^{*}P < 0.05$, $t = 3.871$, $df = 4$, vs control-Cytoplasm group, $^{\#\#}P < 0.01$, $t = 6.02$, $df = 4$, vs control-Nucleus group. Data represent the mean ± S.E.M.

mice ($P < 0.01$, Fig. 4B). Furthermore, differences in Tet2 protein levels in the cytoplasmic and nuclear fractions were detected by western blot analysis. Consistent with the Tet2 immunostaining, Tet2 protein was significantly increased in the cytoplasmic fraction and decreased in the nuclear fraction ($P < 0.01$, 0.001, Fig. 4C and D). These findings suggest that environmental stress can increase total Tet2 protein level, although the nuclear translocation of Tet2 protein from the cytosol is reduced.

Ahi1 protein interacts with TET2 and facilitates Tet2 nuclear translocation

In order to explore how Tet2 protein translocation from the cytoplasm to the nucleus was diminished, we transfected 293T cells with a Tet2 overexpression plasmid and performed immunoprecipitation followed by mass spectrometry using a Tet2 antibody to identify Tet2-interacting proteins. Tet2-interacting proteins were analyzed and were grouped according to the functions as shown in Figure 5A. Gene Ontology analysis indicated that the functions of Tet2-interacting proteins included nuclear transportation, protein folding and vesicle-mediated transport (Fig. 5A and Supplementary Material, Table S2). Interestingly, among the Tet2-interacting proteins, Ahi1 was a protein that was related to protein nuclear transportation. Considering its cellular trafficking functions (32) and that it is a depression-related protein (33), we hypothesized that Ahi1 was a candidate that could potentially facilitate the translocation of Tet2 from the cytoplasm to the nucleus. Therefore, we further examined the Ahi1-Tet2 interaction and confirmed the *in vivo* association between Tet2 and Ahi1 (Supplementary Material, Fig. S3A). Moreover, the colocalization of Ahi1 and Tet2 near the nucleus was confirmed by immunofluorescence staining (Supplementary Material, Fig. S3B).

To investigate the function of Ahi1 on nuclear translocation of Tet2, we cotransfected FLAG-tagged Tet2 plasmid and Ahi1 siRNA plasmid or negative control plasmid in hippocampal HT22 cells. Our immunofluorescence staining showed that Ahi1 knockdown by siRNA increased the cytoplasmic distribution of Tet2 (Fig. 5B). Also, western blot results revealed that Ahi1 knockdown reduced Tet2 protein in the nuclear fraction ($P < 0.01$, Supplementary Material, Fig. S3C). NLS-containing cargo

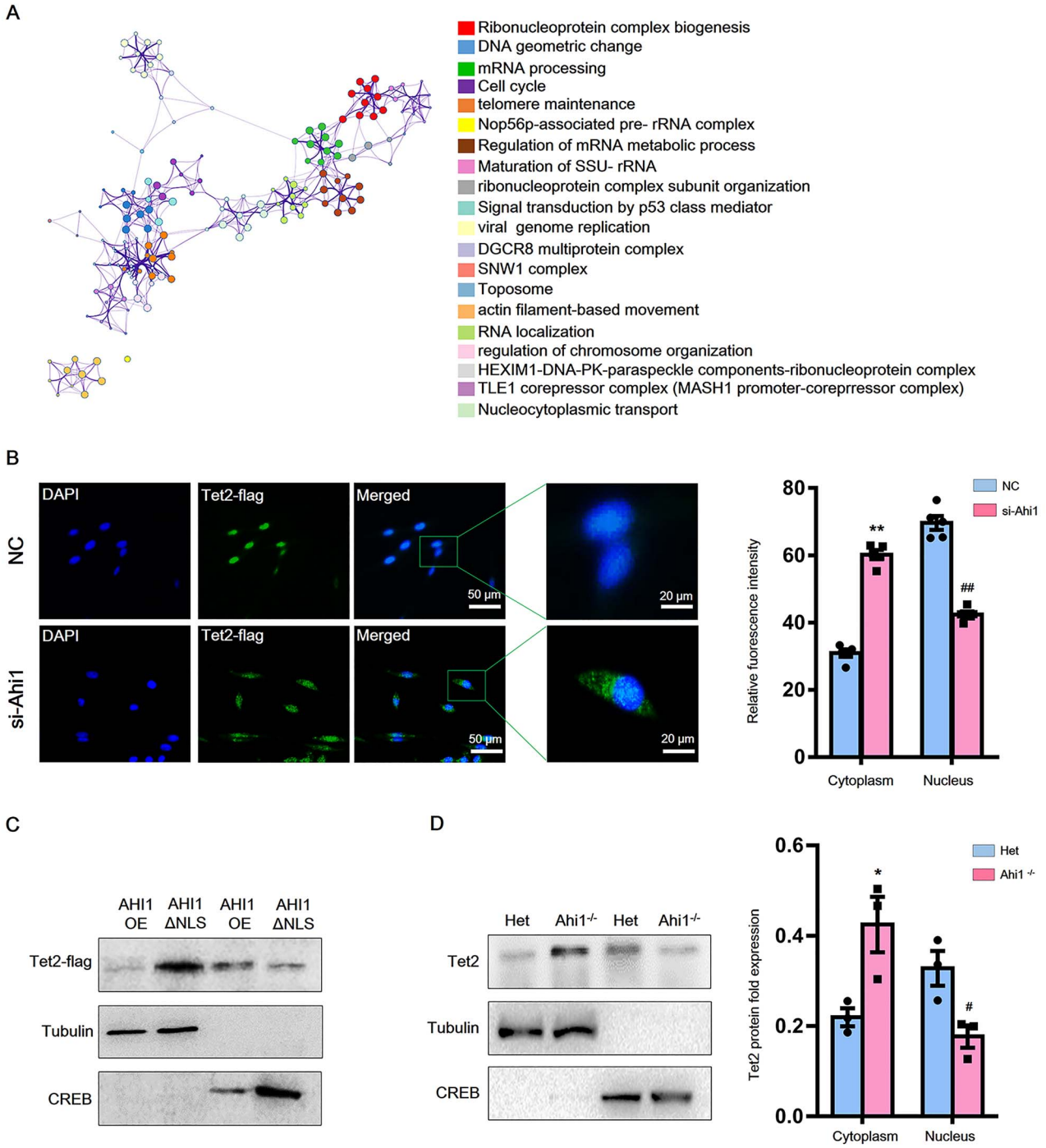

Figure 5. Ahi1 deficiency alters Tet2 nuclear accumulation. (**A**) Network diagram of Tet2 interacting proteins obtained by GO term analysis. GO analysis for identified proteins reveals a strong enrichment for GO terms associated with nuclear transport. (**B**) HT22 cells were cultured for 48h after transfection with Tet2-flag plasmid and negative control si-RNA (NC) or si-Ahi1, and stained for flag (green) and DAPI (blue), revealing Tet2 mislocalization into the cytoplasm in HT22 cells. The data of NC group is represented by dots and si-Ahi1 group is represented by squares. $N = 5$, two-tailed Student's t test, $^{**}P < 0.01$, $t = 16.43$, $df = 8$, vs Het-Cytoplasm group, $^{\#\#}P < 0.01$, $t = 11.98$, $df = 8$, vs Het-Nucleus group. Scale bar, 50 μm (left), 20 μm (right). (**C**) Transient transfection of 293T cells with Ahi1 nuclear localization sequence knockout (Ahi1ΔNLS) plasmid and Tet2-flag plasmid. Separation of the nuclear and cytoplasmic fractions confirms Tet2-flag accumulation in the cytoplasm of Ahi1ΔNLS-transfected cells. Tubulin and CREB served as cytoplasmic and nuclear markers, respectively. (**D**) Separation of the nuclear and cytoplasmic fractions confirms Tet2-flag accumulation in the cytoplasm of hippocampus of Ahi1 knockout mice. Tubulin and CREB served as cytoplasmic and nuclear markers, respectively. The data of Het group is represented by dots and Ahi1-/- group is represented by squares. $N = 3$, two-tailed Student's t test, $^{*}P < 0.05$, $t = 3.177$, $df = 4$, vs Het-Cytoplasm group, $^{\#}P < 0.05$, $t = 3.286$, $df = 4$, vs Het-Nucleus group. Data are expressed as mean ± S.E.M.

molecules can be recognized and transported into the nucleus by the proteins importin-β and importin-α (34). Thus, we used the pharmacologic importin-β inhibitor, Importazole, to inhibit the nuclear import of any protein bearing a classical NLS signal (35). As shown in Supplementary Material, Figure S4, inhibition by Importazole of the nuclear import of Tet2 protein proves that

the nuclear transport of Tet2 protein requires the assistance of an NLS-containing protein and importin-β. Because the nuclear localization signal (NLS) is essential for the nuclear transport of proteins, an Ahi1 plasmid without an NLS (Ahi1-ΔNLS) was transfected into cells. In the absence of the Ahi NLS, Tet2 protein accumulated in the cytoplasm but not in the nucleus ($P < 0.01$, Fig. 5C), indicating the critical role of Ahi1 on Tet2 nuclear translocation. Consistent with our *in vitro* findings, Ahi1 knockout (Ahi1$^{-/-}$) resulted in increased Tet2 levels in cytoplasm but not in the nucleus (Fig. 5D), further supporting our theory that Ahi1 facilitates the nuclear translocation of Tet2. Consistent with the results of our published article (36), our western blot results showed a significant reduction in Ahi1 protein under stress (Supplementary Material, Fig. S3D).

Discussion

Epigenetic mechanisms are reported to have a direct role in the development of persistent depressive behaviors and related psychopathology in patients and are considered as significant factors in the induction of acute and chronic stress exposure (37,38). Recent studies of several neuropsychiatric conditions have focused on 5hmC regulation as the likely trigger of depressive episodes (39,40). Tet enzymes oxidize 5mC into 5hmC, which is enriched in certain brain regions (41) and mediates the response to environmental stress (25). Our present data have demonstrated that Cre-mediated Tet2 knockout or Tet2 knockdown specifically in the hippocampus can induce depression-like behaviors. To further confirm that these depression-like phenotypes were caused by Tet2 deficiency, not Tet2 KO-mediated developmental defects, we intraperitoneally injected tamoxifen in Cre^{ERT2} Tet2$^{fl/fl}$ mice, thereby obtaining Tet2 conditional knockout mice after the mice were born. Our findings together clearly demonstrated that Tet2 is a key epigenetic player that mediates depression-like behaviors in mice.

Intriguingly, overall Tet2 protein levels were significantly increased in the mice that were exposed to stress, while the levels of DNA 5hmC were markedly decreased. We further analyzed the genome-wide distribution of 5hmC using a previously established 5hmC capture method, combined with high-throughput sequencing (25). By investigating the DhMRs, we found that Tet2 CKO resulted in significant loss of 5hmC in many regions, consistent with the global reduction of 5hmC. These results are further supported by a study indicating that 5hmC in leukocyte DNA is significantly reduced in patients with MDD (16). A total of 651 DhMRs induced by Tet2 CKO were identified. After removing empty names and duplicated names, they mapped to 461 unique human genes, 31 of which were associated with depression. KEGG analysis showed that overlapping pathways between Tet2 CKO-induced DhMRs are also strongly enriched in synaptic function. In our additional GO analysis, genes with 5hmC changes caused by Tet2 deletion were significantly involved in synaptic function and axon guidance, which is associated with depression. Tet enzymes and 5hmC were reported to mediate dynamic DNA hydroxymethylation in the hippocampus where they impact neurogenesis and synaptic plasticity (42–44). Our results extend these findings by revealing a previously unappreciated role for Tet2-regulated synaptic function in depression.

Larger proteins often require the carrier protein importins and cargo proteins containing NLS for active transport into the nucleus (45). Increasing evidence supports that transport proteins are intimately involved in neuropsychiatric conditions. For example, variation or elevation of FK506-binding protein 5 (FKBP5), a gene associated with the cytoplasmic/nuclear distribution of GR (46), is thought to contribute to major depression (47); *KPNA3* (also known as importin alpha-4, a critical protein related to protein nuclear translocation) has been linked to schizophrenia, major depression and alcohol dependence (48). Because Tet2-mediated DNA hydroxymethylation modification occurs in the nucleus, the nuclear localization of Tet2 protein from the cytosol after its translation is essential to its function. In this study, we found an abnormal cellular distribution of Tet2 in depressed mice, which explains the two seemingly contradictory phenomena of increased Tet2 in the hippocampus of depressed mice and depression-like behaviors in Tet2 CKO mice. Interestingly, Ahi1, a trafficking protein (32,33), was found to be a Tet2-interacting protein using mass spectrometry and immunoprecipitation. In addition, Ahi1 knockout or knockdown inhibited the translocation of Tet2 from the cytosol to the nucleus, suggesting that the abnormal intracellular localization of Tet2 enzymes by Ahi1 was related to the depression-like behaviors. Our results provide support for the theory that the modulation of Tet2 nuclear translocation could be a highly promising therapeutic target for depression-like behaviors and stress-related diseases. Because there is some debate about the behavioral tests used for their translatability to depression in humans (49,50), these factors should be taken into account for translation into human depression.

In summary, this study has uncovered Ahi1-dependent nuclear translocation of the Tet2 protein in response to stress exposure. Our results highlight the importance of Tet2-dependent 5hmC modifications of DNA in stress-induced depression, which is implicated in various pathways, especially those related to synaptic function. Further understanding the molecular mechanism governing the interaction between Tet2 and the nuclear transport machinery, as well as the role of Ahi1-Tet2 pathways in stress-induced behaviors, is warranted.

Materials and Methods

Animals

All animal procedures were approved by the Institutional Animal Care and Use Committee of Soochow University. In this project, C57BL/6 WT (25.0–30.0 g, 6–8 weeks old) mice were purchased from Shanghai Research Center for Model Organisms. CD1 (ICR) mice (stock number 201, CD-1® (ICR) IGS) were purchased from Charles River.

Tet2$^{flox/flox}$ line was obtained from the Jackson Laboratory (stock number 017573, B6; 129S4-Tet2$^{tm1.1Iaai}$/J). These floxed mutant mice possess loxP sites flanking exon 3 of the Tet2 gene. This strain can be used for the conditional knockout of Tet2 for studying hematopoietic stem cell self-renewal and myeloid transformation. Nestin-Cre mice were obtained from the Jackson Laboratory (stock number 003771, B6. Cg-Tg (Nes-cre) 1Kln/J). The Nestin promotor-driven Cre recombinase is expressed in the central and peripheral nervous system.

Ubc-creERT2 mice (stock number 007179, B6.Cg-Tg (UBC-cre/ERT2) 1Ejb, described as Cre^{ERT2} herein) were also obtained from the Jackson Laboratory (stock number 008085, B6.Cg-Tg (UBC-cre/ERT2)1Ejb/J). Cre^{ERT2} Tet2$^{fl/fl}$ mice were obtained by crossing two generations of Cre^{ERT2} and Tet2 $^{flox/flox}$ mice. Intraperitoneal injection of tamoxifen (Sigma Aldrich, 10540-29-1) was carried out for inducing Cre-driver lines. Tamoxifen was dissolved in corn oil at a concentration of 20 mg/ml by shaking overnight at 37°C. Injection dose was determined by weight,

using approximately 75 mg tamoxifen/kg body weight. For adult mice, a standard dose of 100µl tamoxifen/corn oil solution (above) is effective for inducing recombination. Tamoxifen was administered via intraperitoneal injection (using an ACUC-approved injection procedure) once a day for 5 consecutive days. There is a 7-day waiting period between the final injection and necropsy/histological analysis.

Stereotactic injection of AAV-eGFP and AAV-Cre-eGFP

Mice were given an analgesic via IP injection (ketoprofen, 5 mg/kg), and artificial tears were placed on the eyes of the mouse to prevent drying. We ensured that mice were fully asleep by pinching their foot. If the mouse responded to the foot pinch, more anesthetic was given (in doses of 50 µl). The mouse was then placed onto the stereotactic apparatus and microinjected bilaterally with AAV. The microinjection coordinates were 2.06 mm behind the bregma and ± 1.5 mm lateral from the sagittal midline at a depth of 2 mm from skull surface. Behavioral tests were conducted three weeks after AAV microinjection of the mice.

Chronic mild stress

Mice were exposed to various, randomly scheduled, low-intensity social and environmental stressors 2–3 times a day for 8 weeks. The stressors included the following: (1) food deprivation for 24 h (2), water deprivation for 24 h (3), overnight illumination (4), absence of sawdust in cage for 24 h (5), moistened sawdust with water for 24 h (6), forced swimming at 6°C for 5 min (7), tail pinch (1 cm from the tip of the tail) (8), physical restraint for 2 h and (9) 45° cage-tilt along the vertical axis for 3 h.

Chronic social defeat stress

C57BL/6 WT mice were randomly allocated to two groups: CSDS group and control group. As shown in Supplementary Material, Figure S2A, CSDS and CD1 were housed in a cage that was divided in half by a clear perforated Plexiglas partition that physically separated the mice following 5–10 min defeat sessions. The social defeat was repeated once a day for 10 consecutive days. Control mice were placed in a novel cage for 15 min over 10 consecutive days, and their cages were also equipped with a clear perforated Plexiglas partition.

Behavioral tests

Tail suspension test (TST)

Each mouse is suspended by its tail within its own three-walled rectangular compartment (55 height × 15 width × 11.5 cm depth). During this time, the animal will try to escape and reach for the ground. The time it takes until it remains immobile is measured. Immobility times were determined for 6 min.

Forced swim test (FST)

Each animal is placed in a glass cylindrical container filled with water (maintained at 24 ± 1°C) at a depth of 20 cm. Water is changed between mice. Immobility scores were determined for the entire 6 min of the test.

Sucrose preference test (SPT)

SPT was performed according to a previous report (51). Prior to beginning testing, mice are habituated to the presence of two drinking bottles (one containing 1% sucrose and the other water) for 3 days in their home cage, and the positions of two bottles are switched daily to reduce any confounding produced by a side bias. Following this acclimation, mice have free choice to either drink 2% sucrose solution or plain water. Water and sucrose solution intake are measured after 24 h. Sucrose preference is calculated as a percentage of the volume of sucrose intake over the total volume of fluid intake.

Novelty-suppressed feeding test (NSFT)

NSFT was carried out in an open field measuring 40 × 40 cm. Mice fasted 24 h before the test. The test was begun by placing a single pellet of food on a white paper platform at the center of the box. A mouse was placed in a corner of the maze, and a stopwatch was used for timing. The timer was stopped when the mouse obtained the food using its forepaws and started eating.

Cell lines and cell culture

All cell lines were seeded into culture dishes (10 cm in diameter) and cultivated at 37°C. HT22 and HEK293T (KeyGEN BioTECH, cat# KG405) were cultivated in Dulbecco's modified eagle's medium (DMEM, Gibco, cat# 12100046), 10% fetal bovine serum (FBS), 1% penicillin/streptomycin (SHYUANYE, cat# R200166), 37°C and 5% CO2.

RNA isolation and qRT-PCR

RNA isolation was carried out with RNeasy Plus Mini kit according to the manufacturer's manual. qRT-PCR was performed by using the 7500 real-time PCR machine (Applied Biosystems, USA), as recently described (52). We designed one gene-specific sense primer at the end of the coding sequence of each gene (Supplementary Material, Table S1).

Immunofluorescence

Brain tissue sections were washed three times in PBS and then blocked in PBS containing 5% fetal bovine serum and 0.1% Triton – X 100 for 1 h at room temperature. Primary antibodies were prepared in the same blocking solution and incubated for 24 h at 4°C. The primary antibodies are as follows: Rabbit anti-Tet2 (1: 800, ab124297, Abcam), Goat anti-PSD95 (1: 1000, ab12093, Abcam) and Mouse anti-Ahi1 (1: 500, ab151193, Abcam). After 24 h, the slices were washed 5 times in PBS and then incubated for 1 h at room temperature in Alexa Fluor fluorescent secondary antibody (1:1000 dilution, Life Technologies) prepared in blocking solution. Finally, sections were washed 3 times in PBS, mounted on gelatin-coated slides, and coverslipped with Vectashield mounting media containing DAPI (MBD0015, Sigma Aldrich). Fluorescent images were captured using a (AXIO SCOPE A1, ZEISS) slide-scanning microscope.

Genomic DNA preparation

Mouse hippocampus was dissected from the brain. Genomic DNA was treated with 500 µl of digestion buffer (100 mM Tris-HCl, pH 8.5, 5 mM EDTA, 0.2% SDS, 200 mM NaCl) and Proteinase K (Sangon Biotech, cat# A600451) at 55°C overnight. The second day, samples were placed at 85°C for 45 min. When the sample returned to room temperature, 500 µl of Phenol:Chloroform:Isoamyl Alcohol (25:24:1 Saturated with 10 mM Tris, pH 8.0, 1 mM EDTA) (Sigma-Aldrich, cat# P-3803) was added to samples, mixed completely and centrifuged for 10 min at 14 000 rcf. The aqueous layer solution was then transferred into a new Eppendorf tube and precipitated with

500 µl isopropanol. The pellet was washed three times with 75% ethanol, air-dried and eluted with 20 µl Nuclease-Free Water (Ambion, cat# AM9930).

Dot Blot

A grid was drawn by pencil onto nitrocellulose membrane (Thermo Fisher, cat# LC2001) to indicate regions. Using a narrow-mouth pipette tip, 2 µl of samples were spotted onto the nitrocellulose membrane at the center of the grid. The membrane was dried at room temperature (RT). Non-specific sites were blocked by soaking the membrane in 5% BSA in TBS-T (20 mM Tris-HCl, 150 mM NaCl, pH 7.5, 0.05% Tween20) for 0.5 h at RT. Rabbit antibody to 5hmC (1:10 000, cat# 39769, Active Motif) was used as the primary antibody and was incubated overnight at 4°C. Horseradish peroxidase–conjugated antibody to rabbit (1:5 000, #A-0545, Sigma) was used as a secondary antibody and incubated for 1 h at RT. The membrane was then washed three times with TBS-T (15 min × 1, 5 min × 2) and once with TBS (5 min). Next, the membrane was incubated with ECL reagent (Sangon Biotech, cat# c510043-0100) for 1 min, covered with Saran-wrap (excessive solution was removed from the surface) and exposed to X-ray film in the dark room.

Immunoprecipitation (IP) and western blot analysis

On ice in a microcentrifuge tube, the recommended amount of antibody was added to 10–50 µg of tissue lysate, and the samples were incubated with the antibody for 12 h at 4°C, under gentle agitation or rotation. Tet2 antibody was conjugated with protein G-coupled Sepharose beads. One milliliters of PBS 0.1% BSA was added and mixed for 1 h using an Eppendorf rotator. The sample was then rinsed twice with PBS. The supernatant was removed and 400 µl of buffer made with protease inhibitors was added. The slurry was then mixed well and 70–100 µl of the beads was added to each sample. The lysate bead mixture was incubated at 4°C under rotary agitation for 4 h. The tubes were then centrifuged, and the supernatant was removed from the beads and discarded, with the protein of interest specifically bound to the antibody coating the beads. The beads were washed with washing buffer or lysis buffer three times to remove any non-specific binding. For each wash, the beads were mixed gently with wash buffer and centrifuged at 4°C and the supernatant was discarded. As much wash buffer as possible was carefully removed from the beads. The immunoprecipitates were eluted with 2× Laemmli Sample Buffer (Bio-Rad), boiled at 95°C for 10 min, and western blot assays were carried out.

Mass spectrometry

Potential Tet2-interacting proteins obtained by immunoprecipitation were used for gel electrophoresis, and then the gel bands were used for In-Gel Digestion of Proteins (53). As described in a previous study (54), the lyophilized proteins obtained in the In-Gel Digestion of Proteins step were performed for protein separation by liquid chromatography. Then the isolated proteins were identified by mass spectrometry. The mass spectrometry acquisition parameters are as follows: Spray voltage: 2200 v; Capillary Temperature: 350°C; Ion Source: NSI;Full MS: Resolution: 120 000 FWHM; Full Scan AGC target: 2.0e5; Full Scan Max.IT: 50 ms; Scan range: 250-1450 m/z; dd-MS2: Resolution: 30 000 FWHM; AGC target: 5.0e4; Maximum IT: 50 ms; NCE: 30%. Mass spectrometry data analysis was performed by the publicly available Mascot server. We statistically evaluated the match between the observed and predicted peptides and obtained a peptide score, with higher scores indicating a better match between peptide secondary profiles. According to the principle of Parsimony algorithm (55), the protein is inferred from the correspondence between the amino acid sequences of the peptide and the protein. Protein scores are obtained by weighting the scores of the peptides that make up the protein, with higher protein scores indicating higher confidence.

5hmC-specific chemical labeling, affinity purification and sequencing

5hmC enrichment was performed as previously described (25). Following the Illumina protocol for 'Preparing Samples for ChIP Sequencing of DNA' (Part# 111257047 Rev. A), 20 ng of input genomic DNA or 5hmC-captured DNA were used for DNA libraries preparation. Illumina Hi-seq 2000 machines were used for running sequencing libraries.

Sequence alignment, binning and peak identification

The raw fastq files generated from the high-throughput sequencing machine were aligned to the mouse genome (mm9) using Bowtie2 (version 2.2.6). Non-duplicated reads with unique alignment were retained for downstream analyses (56). High-throughput sequencing resulted in a range from 19 to 31 million non-duplicated reads. The whole mouse genome (mm9) was cut into 500 bp bins, and all bins with genomic features and nearby gene were annotated by Homer (57). For each sample, the mapped read counts in all bins were counted. The DhMR detection was performed by comparing the bin-level read counts between cases and controls using DESeq2 (58), which models the count data using negative binomial models. After accounting for multiple testing, the bins with an adjusted *P*-value smaller than 0.20 was deemed as DhMRs. Gene Ontology and pathway enrichment analysis was performed with EnrichR (59). All data analysis was performed in R 3.6.2 unless otherwise mentioned.

Data analysis

Prism 7.0 (GraphPad Software) was used for data analyses. Datasets were analyzed for significance using either unpaired Student's two-tailed *t* tests or ANOVA with multiple comparison *post hoc* tests; all data are presented as mean ± SEM. Samples and animal groups with P-value < 0.05 were considered statistically significant.

Supplementary Material

Supplementary Material is available at *HMG* online.

Data and Code Availability

We have deposited the high-throughput sequencing data into the Gene Expression Omnibus (GEO) at https://www.ncbi.nlm.nih.gov/geo/. The accession number is GSE167344.

Acknowledgements

This work was supported by the grants from National Key R&D Program of China (2017YFE0103700), National Science Foundation of China (81120108011, 81771454 and 82071511) to Xingshun Xu and National Institutes of Health (R35NS111602) to P.J. The

funders had no role in study design, data collection and analysis, decision to publish, or preparation of the manuscript.

Conflict of Interest statement. The authors declare that they have no conflict of interest.

References

1. Burcusa, S.L. and Iacono, W.G. (2007) Risk for recurrence in depression. *Clin. Psychol. Rev.*, **27**, 959–985.
2. Underwood, M.D., Kassir, S.A., Bakalian, M.J., Galfalvy, H., Dwork, A.J., Mann, J.J. and Arango, V. (2018) Serotonin receptors and suicide, major depression, alcohol use disorder and reported early life adversity. *Transl. Psychiatry*, **8**, 279.
3. Slavich, G.M. and Irwin, M.R. (2014) From stress to inflammation and major depressive disorder: a social signal transduction theory of depression. *Psychol. Bull.*, **140**, 774–815.
4. Rogers, J., Raveendran, M., Fawcett, G.L., Fox, A.S., Shelton, S.E., Oler, J.A., Cheverud, J., Muzny, D.M., Gibbs, R.A., Davidson, R.J. *et al.* (2013) CRHR1 genotypes, neural circuits and the diathesis for anxiety and depression. *Mol. Psychiatry*, **18**, 700–707.
5. Diniz, C., Casarotto, P.C., Resstel, L. and Joca, S.R.L. (2018) Beyond good and evil: a putative continuum-sorting hypothesis for the functional role of proBDNF/BDNF-propeptide/mBDNF in antidepressant treatment. *Neurosci. Biobehav. Rev.*, **90**, 70–83.
6. Navarrete, M., Cuartero, M.I., Palenzuela, R., Draffin, J.E., Konomi, A., Serra, I., Colie, S., Castano-Castano, S., Hasan, M.T., Nebreda, A.R. *et al.* (2019) Astrocytic p38alpha MAPK drives NMDA receptor-dependent long-term depression and modulates long-term memory. *Nat. Commun.*, **10**, 2968.
7. Kawasaki, F. and Ordway, R.W. (2009) Molecular mechanisms determining conserved properties of short-term synaptic depression revealed in NSF and SNAP-25 conditional mutants. *Proc. Natl. Acad. Sci. U. S. A.*, **106**, 14658–14663.
8. Border, R., Johnson, E.C., Evans, L.M., Smolen, A., Berley, N., Sullivan, P.F. and Keller, M.C. (2019) No support for historical candidate gene or candidate gene-by-interaction hypotheses for major depression across multiple large samples. *Am. J. Psychiatry*, **176**, 376–387.
9. Dalton, V.S., Kolshus, E. and McLoughlin, D.M. (2014) Epigenetics and depression: return of the repressed. *J. Affect. Disord.*, **155**, 1–12.
10. Lolak, S., Suwannarat, P. and Lipsky, R.H. (2014) Epigenetics of depression. *Prog. Mol. Biol. Transl. Sci.*, **128**, 103–137.
11. Mateus-Pinheiro, A., Pinto, L. and Sousa, N. (2011) Epigenetic (de)regulation of adult hippocampal neurogenesis: implications for depression. *Clin. Epigenetics*, **3**, 5.
12. Cramer, T., Rosenberg, T., Kisliouk, T. and Meiri, N. (2019) Early-life epigenetic changes along the corticotropin-releasing hormone (CRH) gene influence resilience or vulnerability to heat stress later in life. *Mol. Psychiatry*, **24**, 1013–1026.
13. Alisch, R.S., Chopra, P., Fox, A.S., Chen, K., White, A.T., Roseboom, P.H., Keles, S. and Kalin, N.H. (2014) Differentially methylated plasticity genes in the amygdala of young primates are linked to anxious temperament, an at risk phenotype for anxiety and depressive disorders. *J. Neurosci.*, **34**, 15548–15556.
14. Tozzi, L., Farrell, C., Booij, L., Doolin, K., Nemoda, Z., Szyf, M., Pomares, F.B., Chiarella, J., O'Keane, V. and Frodl, T. (2018) Epigenetic changes of FKBP5 as a link connecting genetic and environmental risk factors with structural and functional brain changes in major depression. *Neuropsychopharmacology*, **43**, 1138–1145.
15. Gross, J.A., Pacis, A., Chen, G.G., Drupals, M., Lutz, P.E., Barreiro, L.B. and Turecki, G. (2017) Gene-body 5-hydroxymethylation is associated with gene expression changes in the prefrontal cortex of depressed individuals. *Transl. Psychiatry*, **7**, e1119.
16. Tseng, P.T., Lin, P.Y., Lee, Y., Hung, C.F., Lung, F.W., Chen, C.S. and Chong, M.Y. (2014) Age-associated decrease in global DNA methylation in patients with major depression. *Neuropsychiatr. Dis. Treat.*, **10**, 2105–2114.
17. Ross, S.E. and Bogdanovic, O. (2019) TET enzymes, DNA demethylation and pluripotency. *Biochem. Soc. Trans.*, **47**, 875–885.
18. Guo, J.U., Su, Y., Zhong, C., Ming, G.L. and Song, H. (2011) Hydroxylation of 5-methylcytosine by TET1 promotes active DNA demethylation in the adult brain. *Cell*, **145**, 423–434.
19. Wang, Y., Liu, B., Yang, Y., Wang, Y., Zhao, Z., Miao, Z. and Zhu, J. (2019) Metformin exerts antidepressant effects by regulated DNA hydroxymethylation. *Epigenomics*, **11**, 655–667.
20. Wei, Y., Melas, P.A., Wegener, G., Mathé, A.A. and Lavebratt, C. (2014) Antidepressant-like effect of sodium butyrate is associated with an increase in TET1 and in 5-hydroxymethylation levels in the Bdnf gene. *Int. J. Neuropsychopharmacol.*, **18**, pyu032.
21. Feng, J., Pena, C.J., Purushothaman, I., Engmann, O., Walker, D., Brown, A.N., Issler, O., Doyle, M., Harrigan, E., Mouzon, E. *et al.* (2017) Tet1 in nucleus accumbens opposes depression- and anxiety-like behaviors. *Neuropsychopharmacology*, **42**, 1657–1669.
22. Rudenko, A., Dawlaty, M.M., Seo, J., Cheng, A.W., Meng, J., Le, T., Faull, K.F., Jaenisch, R. and Tsai, L.H. (2013) Tet1 is critical for neuronal activity-regulated gene expression and memory extinction. *Neuron*, **79**, 1109–1122.
23. Gu, T.P., Guo, F., Yang, H., Wu, H.P., Xu, G.F., Liu, W., Xie, Z.G., Shi, L., He, X., Jin, S.G. *et al.* (2011) The role of Tet3 DNA dioxygenase in epigenetic reprogramming by oocytes. *Nature*, **477**, 606–610.
24. Antunes, C., Da Silva, J.D., Guerra-Gomes, S., Alves, N.D., Ferreira, F., Loureiro-Campos, E., Branco, M.R., Sousa, N., Reik, W., Pinto, L. *et al.* (2020) Tet3 ablation in adult brain neurons increases anxiety-like behavior and regulates cognitive function in mice. *Mol. Psychiatry*, **26**, 1445–1457.
25. Cheng, Y., Sun, M., Chen, L., Li, Y., Lin, L., Yao, B., Li, Z., Wang, Z., Chen, J., Miao, Z. *et al.* (2018) Ten-eleven translocation proteins modulate the response to environmental stress in mice. *Cell Rep.*, **25**, 3194–3203.e3194.
26. Powell, T.R., Fernandes, C. and Schalkwyk, L.C. (2012) Depression-related behavioral tests. *Curr Protoc Mouse Biol.*, **2**, 119–127.
27. Hyde, C.L., Nagle, M.W., Tian, C., Chen, X., Paciga, S.A., Wendland, J.R., Tung, J.Y., Hinds, D.A., Perlis, R.H. and Winslow, A.R. (2016) Identification of 15 genetic loci associated with risk of major depression in individuals of European descent. *Nat. Genet.*, **48**, 1031–1036.
28. Bagot, R.C., Parise, E.M., Peña, C.J., Zhang, H.X., Maze, I., Chaudhury, D., Persaud, B., Cachope, R., Bolaños-Guzmán, C.A., Cheer, J.F. *et al.* (2015) Ventral hippocampal afferents to the nucleus accumbens regulate susceptibility to depression. *Nat. Commun.*, **6**, 7062.

29. Li, Q., Zhang, B., Cao, H., Liu, W., Guo, F., Shen, F., Ye, B., Liu, H., Li, Y. and Liu, Z. (2020) Oxytocin exerts antidepressant-like effect by potentiating dopaminergic synaptic transmission in the mPFC. *Neuropharmacology*, **162**, 107836.
30. Wang, X.L., Yuan, K., Zhang, W., Li, S.X., Gao, G.F. and Lu, L. (2020) Regulation of circadian genes by the MAPK pathway: implications for rapid antidepressant action. *Neurosci. Bull.*, **36**, 66–76.
31. Kurian, J.R., Louis, S., Keen, K.L., Wolfe, A., Terasawa, E. and Levine, J.E. (2016) The methylcytosine dioxygenase ten-eleven translocase-2 (tet2) enables elevated GnRH gene expression and maintenance of male reproductive function. *Endocrinology*, **157**, 3588–3603.
32. Lancaster, M.A., Louie, C.M., Silhavy, J.L., Sintasath, L., Decambre, M., Nigam, S.K., Willert, K. and Gleeson, J.G. (2009) Impaired Wnt-beta-catenin signaling disrupts adult renal homeostasis and leads to cystic kidney ciliopathy. *Nat. Med.*, **15**, 1046–1054.
33. Xu, X., Yang, H., Lin, Y.F., Li, X., Cape, A., Ressler, K.J., Li, S. and Li, X.J. (2010) Neuronal Abelson helper integration site-1 (Ahi1) deficiency in mice alters TrkB signaling with a depressive phenotype. *Proc. Natl. Acad. Sci. U. S. A.*, **107**, 19126–19131.
34. Harel, A. and Forbes, D.J. (2004) Importin beta: conducting a much larger cellular symphony. *Mol. Cell*, **16**, 319–330.
35. Rodriguez-Bravo, V., Pippa, R., Song, W.M., Carceles-Cordon, M., Dominguez-Andres, A., Fujiwara, N., Woo, J., Koh, A.P., Ertel, A., Lokareddy, R.K. *et al.* (2018) Nuclear pores promote lethal prostate cancer by increasing POM121-driven E2F1, MYC, and AR nuclear import. *Cell*, **174**, 1200–1215.e1220.
36. Wang, B., Xin, N., Qian, X., Zhai, L., Miao, Z., Yang, Y., Li, S., Sun, M., Xu, X. and Li, X.J. (2021) Ahi1 regulates the nuclear translocation of glucocorticoid receptor to modulate stress response. *Transl. Psychiatry*, **11**, 188.
37. Mampay, M. and Sheridan, G.K. (2019) REST: an epigenetic regulator of neuronal stress responses in the young and ageing brain. *Front. Neuroendocrinol.*, **53**, 100744.
38. Zannas, A.S. and Chrousos, G.P. (2017) Epigenetic programming by stress and glucocorticoids along the human lifespan. *Mol. Psychiatry*, **22**, 640–646.
39. Papale, L.A., Li, S., Madrid, A., Zhang, Q., Chen, L., Chopra, P., Jin, P., Keles, S. and Alisch, R.S. (2016) Sex-specific hippocampal 5-hydroxymethylcytosine is disrupted in response to acute stress. *Neurobiol. Dis.*, **96**, 54–66.
40. Papale, L.A., Madrid, A., Li, S. and Alisch, R.S. (2017) Early-life stress links 5-hydroxymethylcytosine to anxiety-related behaviors. *Epigenetics*, **12**, 264–276.
41. Tahiliani, M., Koh, K.P., Shen, Y., Pastor, W.A., Bandukwala, H., Brudno, Y., Agarwal, S., Iyer, L.M., Liu, D.R., Aravind, L. *et al.* (2009) Conversion of 5-methylcytosine to 5-hydroxymethylcytosine in mammalian DNA by MLL partner TET1. *Science (New York, N.Y.)*, **324**, 930–935.
42. Li, X., Yao, B., Chen, L., Kang, Y., Li, Y., Cheng, Y., Li, L., Lin, L., Wang, Z., Wang, M. *et al.* (2017) Ten-eleven translocation 2 interacts with forkhead box O3 and regulates adult neurogenesis. *Nat. Commun.*, **8**, 15903.
43. Zhang, R.R., Cui, Q.Y., Murai, K., Lim, Y.C., Smith, Z.D., Jin, S., Ye, P., Rosa, L., Lee, Y.K., Wu, H.P. *et al.* (2013) Tet1 regulates adult hippocampal neurogenesis and cognition. *Cell Stem Cell*, **13**, 237–245.
44. Yu, H., Su, Y., Shin, J., Zhong, C., Guo, J.U., Weng, Y.L., Gao, F., Geschwind, D.H., Coppola, G., Ming, G.L. *et al.* (2015) Tet3 regulates synaptic transmission and homeostatic plasticity via DNA oxidation and repair. *Nat. Neurosci.*, **18**, 836–843.
45. Sorokin, A.V., Kim, E.R. and Ovchinnikov, L.P. (2007) Nucleocytoplasmic transport of proteins. *Biochemistry. Biokhimiia*, **72**, 1439–1457.
46. Lukic, I., Mitic, M., Soldatovic, I., Jovicic, M., Maric, N., Radulovic, J. and Adzic, M. (2015) Accumulation of cytoplasmic glucocorticoid receptor is related to elevation of FKBP5 in lymphocytes of depressed patients. *J. Mol. Neurosci.*, **55**, 951–958.
47. Piechaczek, C.E., Greimel, E., Feldmann, L., Pehl, V., Allgaier, A.K., Frey, M., Freisleder, F.J., Halldorsdottir, T., Binder, E.B., Ising, M. *et al.* (2019) Interactions between FKBP5 variation and environmental stressors in adolescent major depression. *Psychoneuroendocrinology*, **106**, 28–37.
48. Morris, C.P., Baune, B.T., Domschke, K., Arolt, V., Swagell, C.D., Hughes, I.P., Lawford, B.R., Mc, D.Y.R. and Voisey, J. (2012) KPNA3 variation is associated with schizophrenia, major depression, opiate dependence and alcohol dependence. *Dis. Markers*, **33**, 163–170.
49. Reardon, S. (2019) Depression researchers rethink popular mouse swim tests. *Nature*, **571**, 456–457.
50. Molendijk, M.L. and de Kloet, E.R. (2015) Immobility in the forced swim test is adaptive and does not reflect depression. *Psychoneuroendocrinology*, **62**, 389–391.
51. Liu, M.Y., Yin, C.Y., Zhu, L.J., Zhu, X.H., Xu, C., Luo, C.X., Chen, H., Zhu, D.Y. and Zhou, Q.G. (2018) Sucrose preference test for measurement of stress-induced anhedonia in mice. *Nat. Protoc.*, **13**, 1686–1698.
52. Wang, B., Zhang, Y., Dong, H., Gong, S., Wei, B., Luo, M., Wang, H., Wu, X., Liu, W., Xu, X. *et al.* (2018) Loss of Tctn3 causes neuronal apoptosis and neural tube defects in mice. *Cell Death Dis.*, **9**, 520.
53. Lazarev, A.V., Rejtar, T., Dai, S. and Karger, B.L. (2009) Centrifugal methods and devices for rapid in-gel digestion of proteins. *Electrophoresis*, **30**, 966–973.
54. Van Damme, T., Lachová, M., Lynen, F., Szucs, R. and Sandra, P. (2014) Solid-phase extraction based on hydrophilic interaction liquid chromatography with acetone as eluent for eliminating matrix effects in the analysis of biological fluids by LC-MS. *Anal. Bioanal. Chem.*, **406**, 401–407.
55. Zhang, B., Chambers, M.C. and Tabb, D.L. (2007) Proteomic parsimony through bipartite graph analysis improves accuracy and transparency. *J. Proteome Res.*, **6**, 3549–3557.
56. Langmead, B. and Salzberg, S.L. (2012) Fast gapped-read alignment with Bowtie 2. *Nat. Methods*, **9**, 357–359.
57. Heinz, S., Benner, C., Spann, N., Bertolino, E., Lin, Y.C., Laslo, P., Cheng, J.X., Murre, C., Singh, H. and Glass, C.K. (2010) Simple combinations of lineage-determining transcription factors prime cis-regulatory elements required for macrophage and B cell identities. *Mol. Cell*, **38**, 576–589.
58. Love, M.I., Huber, W. and Anders, S. (2014) Moderated estimation of fold change and dispersion for RNA-seq data with DESeq2. *Genome Biol.*, **15**, 550.
59. Chen, E.Y., Tan, C.M., Kou, Y., Duan, Q., Wang, Z., Meirelles, G.V., Clark, N.R. and Ma'ayan, A. (2013) Enrichr: interactive and collaborative HTML5 gene list enrichment analysis tool. *BMC Bioinformatics*, **14**, 128.